Possible egg masses from amphibians, gastropods, and insects in mid-Cretaceous Burmese amber.

Lida Xing [1, 2 #*], Gang Li [3], Ryan C. McKellar [4, 5], Donghao Wang [2 #], Ming Bai [6], Huarong Chen [7], Susan E. Evans [8 #*]

1 State Key Laboratory of Biogeology and Environmental Geology, China University of Geosciences, Beijing 100083, China.

2 School of the Earth Sciences and Resources, China University of Geosciences, Beijing 100083, China.

3 Institute of High Energy Physics, Chinese Academy of Science, Beijing 100049, China

4 Royal Saskatchewan Museum, Regina, Saskatchewan S4P 4W7, Canada

5 Biology Department, University of Regina, Regina, Saskatchewan S4S 0A2, Canada

6 Key Laboratory of Zoological Systematics and Evolution, Institute of Zoology, Chinese Academy of Sciences, Beijing 100101, China

7 Dexu Institute of Palaeontology, Chaozhou 521000, China

8 Department of Cell and Developmental Biology, University College London, London WCIE 6BT, UK

# These authors contributed equally to this work.

Corresponding authors: xinglida@gmail.com; s.e.evans@ucl.ac.uk.

Abstract

The eggs of fish, amphibians, and many invertebrates are soft, delicate structures that are only rarely preserved in the fossil record. Here we report egg masses preserved as inclusions in mid-Cretaceous amber deposits of Myanmar. Of five specimens recovered, three of the egg masses probably pertain to insects, but the other two appear different. One mass is composed of relatively stiff eggs that retain their shape throughout the mass and may be linked by mucoid strands. This morphology resembles that of some terrestrial molluscs. The second mass is composed of softer eggs that have compressed one another so that their shapes are strongly distorted within the mass. These eggs most closely resemble those of amphibians. Given the forest environment reconstructed for the amber locality, the eggs were presumably attached on or close to the resin producing tree.

Keywords:

Myanmar, fossil eggs, Anura, Mollusca, Insecta, Mesozoic

Amber, or fossilized tree resin, is especially beneficial for the preservation of small and soft-bodied organisms. It preserves a wide range of insects, but also soft tissues in three dimensions and with unmatched detail. This has recently provided insights on problematic structures such as open-rachis feathers[1], and examples of structures seldom preserved in other settings, such as snail tentacles[2]. The amber deposits of Northern Myanmar provide a unique record of a coastal tropical forest ecosystem during the mid-Cretaceous[3]. These amber deposits have yielded a diverse assemblage of invertebrates (e.g., insects, spiders, and snails) and plants (e.g., mosses, fungi, ferns, angiosperms and gymnosperms), which have recently been summarized[4]. In recent years, rare vertebrate inclusions have also been recovered, including lizards[5], birds[6-8], a non-avian dinosaur[9], frogs[10], an albanerpetontid amphibian[5,11], and snakes[12].

In 2016, we recovered five amber specimens from Northern Myanmar containing clusters of eggs, clearly from more than one taxon. Based on biostratigraphic evidence (ammonites and palynology), Burmese amber has been dated to the late Albian–Cenomanian (about 105 to 95 million years before present)[13-14]. The U-Pb dating of zircons from the volcaniclastic matrix of the

amber gave a refined age estimate of 98.8 ± 0.6 million years[15].

Results

The amber specimens from the Angbamo area, Tanai Township, Myitkyina District, Kachin Province in northern Myanmar are catalogued as DIP-V-16122 (Figs. 1A, 2A, 3, 4), DIP-CH-17227 (Figs. 1B, 2B, 5), DIP-V-17160 (Fig. 6A–C), DIP-V-17234 (Fig. 6D) and DIP-V-18106 (Fig. 6E). For the size of specimens and egg masses, weights, and the number of eggs, see Table 1. The original specimens are housed in the Dexu Institute of Palaeontology (=DIP), Chaozhou, China.

Morphological type 1

There are 55 eggs in DIP-V-16122, with the smallest having a diameter of 0.84 mm, the largest 1.50 mm, and an average diameter of 1.14 mm (Fig.2A). Each egg comprises a gelatinous mass with a dark central body that probably represents the original ovum (pigmented embryo and yolk). As seen from the synchrotron data (Figs. 2A, 3), this mass of eggs forms a compact three-dimensional cluster, with the eggs closely packed. On their external surfaces, the eggs are round to ovoid in shape (long axis/short axis 1.03–1.38, very close to spherical) but within the mass, as viewed through the synchrotron slice data (Fig. 3), the eggs are seen to be compressed into one another and strongly distorted. The internal fill of each egg is homogenous but each contains a small, spherical cavity (rarely two) that lies close to one of the surfaces (small black arrows in Fig.3B,C). It is possible that this cavity corresponds to the original ovum (dark central body seen in the original specimen), but this is difficult to confirm. At one end of the egg mass (Fig.3C-E), the eggs appear to be desiccated and husk-like, with many broken capsular surfaces. However, none of the eggs is completely empty and has a more or less preserved gelatinous mass. This area of the egg mass is also mixed with carbonized plant debris and impurities. Based on flow lines within the surrounding amber (Fig. 7), it seems as though the egg mass and adjacent fragments of plant material dropped into a pre-existing resin layer. The shriveled eggs in this region may be due to minor exposure and drying before a subsequent resin flow fully encapsulated the egg mass.

It is worth noting that there is also fibrous material around the eggs (Fig. 4A-C). Some of the fibrous material scattered on some surfaces of the egg mass may be fungal hyphae[16-17]. The loose

arrangement of branched fibres is consistent with the morphology of fungal hyphae[16-18], and the varying length and the fixed diameter (around 10μm) also fits the characteristics of hyphae (Fig. 4B and C). Fungal infections (such as water moulds) can occur on modern amphibian eggs and affect the hatching rate[17-21]. The condition in the amber specimen is similar to that observed in infected modern samples[17,20].

Morphological type 2

There are 35 eggs in DIP-CH-17227 (Fig. 1B, 2B, 5), with the smallest having a diameter of 0.66 mm, the largest being 0.99 mm, and the average diameter being 0.83 mm. Like the objects in DIP-CH-16122, the eggs consist of a gelatinous body with a dark central portion, and they are grouped into a three-dimensional mass. However, there are several differences between DIP-CH-16122 and DIP-CH-17227. First, the individual eggs in DIP-CH-17227 hold their round shape both externally and deeper in the egg mass. Secondly, each egg has one, or often two, small extensions so that in some views (e.g., as indicated for some eggs by small black arrows in Fig. 5A), the egg resemble an inflated balloon with a short neck. Thirdly, none of the eggs appears hollow or husk-like, but several on the outer edges have wrinkled surface texture (some strongly so, see asterisks in Fig.5A) with a solid internal fill, a combination that is not seen in the desiccated eggs of DIP-CH-16122. Finally, a majority of the eggs in DIP-CH-17227 have an internal structure of symmetrical or asymmetrical concentric laminae, sometimes with separation of those laminae. Adjacent to the egg mass, is a second group of smaller, pellet-like structures (Fig.1B, 5C, D) that appear to be insect frass (feces).

Morphological type 3

DIP-V-17160 (Fig. 6A–C) contains a flat mass of 28 well separated eggs. The eggs are larger than those in DIP-V-16122 and DIP-CH-17227, at 1.0–1.5 mm in long axis and 0.4–0.8 mm in short axis. DIP-V-17234 (Fig. 6D) contains 18 eggs, of 1.0–1.7 mm in long axis and 0.4–0.8mm in short axis. DIP-V-17160 and, especially, DIP-V-17234 appear to be at a late stage of embryonic development with clearly visible embryos. DIP-V-18106 contains 22 eggs (Fig. 6E), of long axis 0.9–1.4 mm and short axis 0.5–0.7mm. The outer capsules in DIP-V-17160, DIP-V-17234 and DIP-V-18106 are relatively undistorted, and are also more elliptical than those described above, with the proportions of the long axis to the short axis in the range of 1.74–2.68. Eggs in all three

amber pieces have a sheet-like arrangement, with the long axes of the eggs trending away from each other to create a herringbone-like pattern. The surrounding amber is composed of multiple resin flows and the egg sheets are nearly parallel to these flow lines. Fine particulates are concentrated within the surrounding amber, toward the presumed base of each egg layer.

Discussion

DIP-V-17160 (Fig. 6A–C), DIP-V-17234 (Fig. 6D), and DIP-V-18106 (Fig.6E) resemble the eggs of modern insects in being oval with a firm capsule (chorion) and large embryo (hook-like in DIP-V-17160). In these elliptical eggs, the proportions of the long axes to the short axes (1.64–2.68) are comparable to the proportions in living coleopterans, such as *Sternoplax souvorowiana* (~ 2.0[22]). The chorions of the amber-entombed eggs show no signs of external sculpture related to pores, micropyles, or opercula. This lack of detail may be due to resin infilling fine structures within the chorion and reducing contrast in both visual and X-ray observations, but some of these details have been observed in other amber deposits[23]. The larvae within may be vermiform, as they lack developed legs or head capsules; however, they may just be in early embryological stages[24]. All three samples have eggs that are preserved in a sheet that extends parallel to repetitive flow lines within the surrounding resin. It is unclear whether the particulates that surround each sheet are due to the eggs drifting off their substrate when they were entrained in a resin flow, or if the particulates were trapped within a jelly or adhesive layer that surrounded the egg mass. Drift from the initial substrate seems to be the most likely scenario given that all three samples include no traces of substrate, and that DIP-V-17234 has dark, highly oxidized drying lines between resin flows that are consistent with prolonged exposure between flows. The absence of preserved substrate, combined with the indeterminate taxonomic placement and developmental stage of the insect eggs in Burmese amber limits the ecological inferences that can be drawn from these samples.

In external appearance, the eggs in DIP-V-16122 and DIP-CH-17227 differ from those attributed to insects—they are rounded rather than elliptical and form a layered three-dimensional mass instead of a sheet. In these features, they more closely resemble amphibian egg masses. In amphibians, one or more jelly layers are laid down around each egg cell (ovum) as it passes

through the oviduct[25]. This jelly facilitates fertilization and protects the egg once it is deposited, varying in physical structure (e.g., toughness, density, thickness, moisture content) depending on the species and the environment of deposition[26]. However, a mass of snail or slug eggs can be similar in size and three-dimensional organization to that of anurans. Furthermore, the eggs of some molluscan genera also have transparent layers. In water, snail eggs may be enclosed in a further common jelly coat, but on land they more often form a clump of well separated, turgid eggs that are often enclosed in a distinct, sometimes calcified, capsule[27,28]. Slug eggs, like some frog eggs (e.g., *Ascaphus*[29]), may be linked together by mucoid strands to form a bead-like string. Internally, each egg is reported to comprise several concentric layers of mucopolysaccharide gel surrounding the ovum and its albumen coat[30-33]. The eggs in DIP-CH-17227 retain their shape within the egg mass, suggesting they were relatively compact and firm, with a resistant capsule. This is supported by the observation that although several of the eggs on the periphery of the mass have strongly wrinkled surfaces, they have not broken open and the interiors remain dense (Fig. 1B, 5A). It seems likely that the wrinkling was caused by dehydration during the resin inclusion process, and is not the result of surface ornamentation or pore structures in an outer chorion (external characteristics of insect eggs). Most of the eggs show evidence of multiple internal layering. Moreover, the short processes seen in DIP-CH-17227 may indicate the eggs were linked by cords of mucoid tissue. All of these features are consistent with the eggs of terrestrial molluscs. The eggs are also small compared to those of frogs. In a list of egg sizes for 383 anuran species[34], only 2.3% of which had an egg in the size range of those within DIP-CH-17227 (0.66–0.99 mm). On balance, we consider it more likely that the eggs within DIP-CH-17227 are gastropod eggs (slug or land snail) rather than anuran or insect eggs. Eggs from gastropods are rare within the Cretaceous fossil record, with only two published reports to date[35]; we were unable to find any definitive reports from amber. Habitats for previous discoveries of gastropod eggs have included soft-shelled eggs in Jurassic and Cretaceous deltaic and marine deposits, and Miocene freshwater deposits, as well as calcareous eggs from land snails in the Paleogene and Neogene[35,36] .

Although the eggs in DIP-V-16122 appear rounded at the exterior surface, they are very distorted and squashed within the egg mass, suggesting they were much softer than the other eggs examined. This arrangement matches the description of a ‘melded clump’ where individual eggs

are separate but have sagged into one another [37]. The spheroidal cavities within these eggs may represent the original ova within the enveloping gelatinous capsular layers, although this is speculative. At one end of the mass, there are many broken, husk-like eggs with severely damaged capsules (Fig 3D). This could again be due to desiccation, or damage due to infection. A study of the egg masses of the myobatrachid *Mixophyses*[38] found that many egg masses contained a small number of rotting, presumably unfertilized or non-viable eggs infected by bacteria or fungi. Such eggs may subsequently shrivel and crack, leading to damage of their capsular membranes. If we are correct in identifying mould around this egg mass, it may explain the husk-like eggs.

The amphibian ovum is often pigmented, at least at the animal pole, and forms a dark body at the center of the egg unit. With a few exceptions (e.g., *Alytes, Discoglossus, Pipa*), frog eggs differ from salamander eggs in this central positioning of the ovum. In salamanders, the mucoid layer closest to the ovum liquidizes within a capsular chamber, so that the embryo has a greater freedom of movement[25]. Given the apparently much softer consistency of the eggs in DIP-V-16122, and their external appearance in the amber block, it seems plausible that the egg mass DIP-V-16122 belonged to an anuran. If so, it must have been deposited on, or at the base of, the resin producing tree, generally considered to be *Metasequoia*[39] or a member of Araucariaceae[40]. It is unlikely that this preservation would have occurred in water, although marine and brackish taxa have been reported from the deposit[3,41]. Instead, flow lines within the surrounding resin (Fig. 7) suggest that the egg mass and leaf fragment entered the resin subaerially, and one side of the egg mass was located near the surface of the resin mass while parts of the leaf weathered away. The surrounding amber lacks dense particulates or arthropod inclusions that would suggest formation on the forest floor.

The eggs of DIP-V-16122 are small, but amphibian eggs can show great intraspecific variation in size. Of the 383 anuran species listed by Summers et al.[34], 13% had eggs in the same size range as those of DIP-V-16122 (0.84–1.14mm). The majority of these species lay their eggs in water, which does not match well with the preservation observed in DIP-V-16122. However, the water bodies used can be ephemeral (e.g., leaf axils in tree frogs), which may explain the fragmentary plant material stranded in the flow line adjacent to the egg mass in DIP-V-16122. Although some very small frogs lay comparatively large eggs (e.g., *Brachycephalus ephippium*,

12.5–19.7 snout to vent length (SVL), with a few large eggs of 5.2 mm in diameter), no significant association between female body size and egg size has been found[34]. Thus, small eggs are not necessarily correlated with small adults.

Clutch sizes in frogs also vary greatly depending on the species and the size of the egg. Arrangement and size of the eggs are helpful when determining the egg-layer, because each species has a unique spawning pattern[37]. These spawning patterns are embodied by five main arrangements in anurans: 1) independent eggs; 2) three-dimensional arrangements; 3) floating eggs; 4) froth nests; and 5) linear arrangements. The three-dimensional arrangement can be divided into clump and mass types, and DIP-V-16122 most closely corresponds to the 'melded clump' type[37]. Among extant frogs, representative taxa producing three-dimensional clumps include many ranids and some tree frogs (e.g., *Phyllomedusa,* and *Pachymedusa*)[37]. However, the evolutionary radiation that increased the diversity and specialization of frogs is not thought to have occurred until the Cretaceous-Paleogene boundary[42]. Nonetheless, if the egg-layer for DIP-V-16122 is anuran, it is likely to represent similar reproductive behaviour and some aspects of life style to extant forest-living frogs.

Among the vertebrates recovered within the Burmese amber were four anuran specimens[10]. These frogs, similar to extant members of the Alytidae or Bombinatoridae, are quite small. The holotype of *Electrorana limoae* (DIP-L-0826) was the largest, having a snout-pelvis length (SPL) of only 22 mm. *Electrorana* provides the oldest definitive evidence of the relationship between anurans and tropical forests, foreshadowing the great diversity of frogs in these habitats today[10]. The holotype specimen of *Electrorana* had undergone complete metamorphosis, but had features indicating immaturity, such as incompletely ossified carpals and sphenethmoid[10]. This level of skeletal development is consistent with that described for the metamorphs of several extant species[43,44]. It is therefore difficult to predict the size at which *Electrorana* might have reached sexual maturity (e.g., *Pyxicephalus adspersus*: metamorph 22.4 mm SVL, female at sexual maturity ~100mm SVL[44], *Bombina:* metamorph 17 mm SVL, female at sexual maturity ~56 mm SVL; *Ascaphus truei*: metamorph 26 mm SVL, female at sexual maturity, 56 mm SVL[45]: With the data that is currently available, we cannot demonstrate that the egg-layer of DIP-V-16122 was *Electrorana*, but the source animal would have shared the same habitat. The only other known

amphibian in Burmese amber is a small specimen originally identified as a lizard[5], but recently shown to belong to the enigmatic terrestrial amphibian clade Albanerpetontidae[11]. However, nothing is currently known of the reproductive habits of these tiny terrestrial amphibians.

The paleoecological environment of China's Jehol biota, which may hold the greatest number of Cretaceous fossil anurans[46], is characterized by lacustrine and open forest habitats. Other deposits that are rich in anurans include the Brazilian Lower Cretaceous Crato Formation, which yields specimens from lacustrine deposits, located in an otherwise semi-arid environment[47]; and the Lower Cretaceous deposits of Las Hoyas, Spain, which represent a wetland habitat[48,49]. These environments are all associated with low-energy freshwater environments, including floodplains and swamps[5]. The eggs described herein are from a tropical rainforest environment in Myanmar, and like the body fossils of frogs from the deposit[10], they shed light on additional habitats occupied during the Cretaceous. Burmese amber was produced by trees marginal to inland and coastal fluvial environments[13], representing a different set of habitats than those sampled by the compression fossil record of anurans.

Conclusions

Soft-shelled eggs are rarely preserved as fossils, but amber offers a unique glimpse of this life stage. Herein, eggs trapped in amber from the mid-Cretaceous of Myanmar are interpreted as belonging to insects, terrestrial gastropods (snails or slugs), and possibly anuran amphibians. The former eggs are not surprising given the diversity of insects known from Burmese amber, some of which are preserved in intimate association with their parents[50]. The latter are the first fossil record of amphibian eggs deposited in amber. They are unique in that they must have been laid within an essentially terrestrial forest environment, either on a tree or at the base of a tree, in order to become engulfed in resin. They represent a different habitat than the majority of previous fossil records for anurans. Similarly, if the gastropod eggs described herein are correctly attributed, they are the first records from amber, and also the first from a terrestrial habitat in the Mesozoic. Hopefully these findings will spur additional collection and recognition of eggs in amber, which may help to resolve some of the questions associated with the currently available specimens.

Methods

DIP-V-16122, DIP-CH-17227 and DIP-V-17160 were imaged non-destructively using PPC-SRX-μCT on the beamline 13W of the Shanghai Synchrotron Radiation Facility (SSRF). The SR beam was monochromatized at 22 keV using the double Si (111) crystal monochromator. The distance between sample and detector (propagation distance) was 60 mm to obtain phase contrast. The physical pixel size of the CCD sensor was 6.5 μm x 6.5 μm and a 2x microscope objective was used, so the isotropic voxel size was 3.25 μm. The pixel number of our detector was 2048 x 2048, and its dynamic range was 16 bits. The field of the view of the detector was 6.5 mm x 6.5 mm. The exposure time of a single projection was 0.3 s and there were 1440 projections. Two scans were performed in a vertical direction as the vertical axis of the specimen was larger than the FOV of our detector.

The phase retrieval and slice reconstruction of all six projection data sets was performed using PITRE-3 software[51]. After the reconstruction, the two segmented CT slice sets were stitched in the vertical direction. Image segmentation allowed the surrounding amber and all included impurities to be filtered out of the data set. Therefore, only the egg data was selected as the region of interest. The sample orientation was adjusted carefully to give the best view to show important information. The rotation correction was performed using ImageJ software. The 3-D data processing, segmentation, and analysis was performed using VG StudioMax 1.2 and 2.1.

The CT datasets generated during and/or analysed during the current study are available from corresponding author (LD) on reasonable request.

References

1. Xing, L. D., Cockx, P., McKellar, R. C. & O'Connor, J. K. Ornamental feathers in Cretaceous Burmese amber: resolving the enigma of rachis-dominated feather structure. *J. Palaeogeogr.* **7**, 13; 10.1186/s42501-018-0014-2 (2018).
2. Xing, L. D., Ross, A. J., Stilwell, J. D., Fang, J. & McKellar, R. C. Juvenile snail with preserved soft tissue in mid-Cretaceous amber from Myanmar suggests a cyclophoroidean (Gastropoda) ancestry. *Cretaceous Res*. **93**, 114–119 (2019).
3. Xing, L. D. *et al*. A gigantic marine ostracod (Crustacea: Myodocopa) trapped in mid-Cretaceous Burmese amber. *Sci. Rep.-UK* **8**, 1365; 10.1038/s41598-018-19877-y (2018).

4. Ross, A. J. Burmese (Myanmar) amber taxa, on-line checklist v.2018.2.104pp. http://www.nms.ac.uk/explore/stories/natural-world/burmese-amber (2018).
5. Daza, J. D., Stanley, E. L., Wagner, P., Bauer, A. M. & Grimaldi, D. A. Mid-Cretaceous amber fossils illuminate the past diversity of tropical lizards. *Science Adv*. **2**, e1501080; 10.1126/sciadv.1501080 (2016).
6. Xing, L. D. *et al.*. Mummified precocial bird wings in mid-Cretaceous Burmese amber. *Nat. Commun*. **7**, 12089; 10.1038/ncomms12089 (2016)
7. Xing, L. D. *et al*. A mid-Cretaceous enantiornithine (Aves) hatchling preserved in Burmese amber with unusual plumage. *Gondwana Res*. **49**, 264–277 (2017).
8. Xing, L. D. *et al.*. A flattened enantiornithine in mid-Cretaceous Burmese amber: morphology and preservation. *Sci. Bull.* **63**, 235–243 (2018)
9. Xing, L. D. *et al*. A feathered dinosaur tail with primitive plumage trapped in mid-Cretaceous amber. *Curr. Biol*. **26**, 3352–3360 (2016).
10. Xing, L. D., Stanley, E., Bai, M. & Blackburn, D. C. The earliest direct evidence of frogs in wet tropical forests from Cretaceous Burmese amber. *Sci. Re.-UK* **8**, 8770; 10.1038/s41598-018-26848-w (2018).
11. Matsumoto, R. & Evans, S. E. The first record of albanerpetontid amphibians from the Early Cretaceous of Japan. *PLoS One* 13, e0189767; 10.1371/journal.pone.0189767 (2018)
12. Xing, L. D. et al. . A mid-Cretaceous embryonic-to-neonate snake in amber from Myanmar. *Sci. Adv.* **4**, eaat5042; 10.1126/sciadv.aat5042 (2018)
13. Cruickshank, R. D. & Ko, K. Geology of an amber locality in the Hukawng Valley, Northern Myanmar. *J. Asian Earth Sci*. **21**, 441–455 (2003).
14. Ross, A., Mellish, C., York, P. & Crighton, B. Burmese amber in *Biodiversity of Fossils in Amber from the Major World Deposits* (ed. Penney, D.) 208-235. (Siri Scientific Press, 2010)
15. Shi, G. H. *et al*. Age constraint on Burmese amber based on U-Pb dating of zircons. *Cretaceous Res*. **37**, 155-163 (2012).
16. Humber, R. A. Fungi: identification in *Manual of Techniques in Insect Pathology* (ed. Lacey, L. A.) 153-185. (Academic Press 1997).
17. Lee, B., Longcore, J. E., Speare, R., Hyatt, A. & Skerratt, L. F. Fungal diseases in amphibians in *Amphibian Decline: Diseases, Parasites, Maladies and Pollutions. Amphibian Biology,* 8 (eds. Heatwole, H. & Wilkinson, J. W.) 2986–3052 (Surrey Beatty & Sons, Australia, 2009).
18. Pazouki, M. & Panda, T. Understanding the morphology of fungi. *Bioprocess Eng.* **22**, 127–143 (2000).
19. Blaustein, A. R., Hokit, D. G. & O'Hara, R. K. Pathogenic fungus contributes to amphibian losses in the Pacific Northwest. *Biol. Conserv*. **67**, 251–254 (1994).
20. Warkentin, K. M., Currie, C. R. & Rehner, S. A. Egg-killing fungus induces early hatching of red-eyed treefrog eggs. *Ecology* **82**, 2860–2869 (2001).
21. Sagvik, J., Uller, T., Stenlund, T. & Olsson, M. Intraspecific variation in resistance of frog

eggs to fungal infection. *Evol. Ecol*. **22**, 193–201 (2008).

22. Wang, Y., Ma, J., Liu, X.N. & Luo, J. M. Egg morphology and chorionic ultrastructures of the desert insect *Sternoplax souvorowiana* (Coleoptera :Tenebrionidae). *Xinjiang Agr. Sci*. **47**, 1703–1708 (2010).
23. Pérez-de la Fuente, R., Engel, M. S., Azar, D. & Peñalver, E. The hatching mechanism of 130-million-year-old insects: an association of neonates, egg shells and egg bursters in Lebanese amber. *Palaeontology* 2018; 10.1111/pala.12414 (2018).
24. Strand, M. The egg and embryology in *The Insects: Structure and Function* (eds. Simpson, S., Douglas, A. 347–397 (Cambridge University Press, 2012)
25. Salthe, S. N. The egg capsules in the Amphibia. *J. Morphol*. **113**, 161–171 (1963).
26. Shu, L.F., Suter, M.J.F., Rasanen, K.. Evolution of egg coats: linking molecular biology and ecology. *Mol. Ecol*. **24**, 4052–4073 (2015).
27. Tompa, A. S. A comparative study of the ultrastructure and mineralogy of calcified land snail eggs (Pulmonata: Stylommatophora). *J. Morphol*. **150**, 861–888 (1976).
28. Baur, B. Parental care in terrestrial gastropods. *Experientia* **50**, 5–14 (1994).
29. Wernz, J. G. & Storm, R. M. Pre-hatching stages of the tailed frog, *Ascaphus truei* Stejneger. *Herpetologica* **25**, 86–93 (1969).
30. Carrick, R. The life history and development of *Agriolomax agrestis* L., the grey field slug. *T. Roy. Soc. Edin.* **59**, 563–579 (1939).
31. Creek, G. A. The reproductive system and embryology of the snail *Pomatias elegans* (Muller) *P. Zool. Soc. Lond.* **121**, 599–639 (1951).
32. Bayne, C.J. Observations on the composition of the layers of the egg of *Agriolimax reticulatus*, the grey field slug (Pulmonata, Stylomatophora). *Comp. Biochem. Physiol*. **19**, 317–338 (1966).
33. Burton, D.W. Anatomy, histology and function of the reproductive system of the trachiopulmonate slug *Athoracophorus bitentaculatus* (Quoy and Gaimand). *Zool. Pub. Victoria Univ. Wellington*, **68**, **69**, **70** (1978).
34. Summers, K., Sea McKeon, C. & Heying, H. The evolution of parental care and egg size: a comparative analysis in frogs. *P. Roy. Soc. B-Biol. Sci.* **273**, 687–692 (2006).
35. Zatoń, M., Mironenko, A. A. & Banasik, K. Gastropod egg capsules from the Lower Cretaceous of Russia preserved by calcitization. *Palaeogeogr. Palaeocl*. **466**, 326–333 (2017).
36. Zatoń, M., Taylor, P. D. & Jagt, J. W. Late Cretaceous gastropod egg capsules from the Netherlands preserved by bioimmuration. *Acta Palaeontol. Pol*. **58**, 351–356 (2012).
37. Altig, R. & McDiarmid, R. W. Morphological diversity and evolution of egg and clutch structure in amphibians. *Herpetol. Monogr*. **21**, 1–32 (2007).
38. Knowles, R. *et al*. Oviposition and egg mass morphology in barred frogs (Anura: Myobatrachidae: *Mixophyes* Günther, 1864), its phylogenetic significance and implications

for conservation management. *Aust. Zool.* **37**, 381–402 (2014).

39. Grimaldi, D. A., Engel, M. S. & Nascimbene, P. C. Fossiliferous Cretaceous amber from Myanmar (Burma): its rediscovery, biotic diversity, and palaeontological significance. *Am. Mus. Novit.* **1956**, 1–72 (2002).
40. Poinar Jr, G., Lambert, J. B. & Wu, Y. Araucarian source of fossiliferous Burmese amber: spectroscopic and anatomical evidence. *J. Bot. Res. Inst. Texas* **1**, 449-455 (2007).
41. Smith, R. D. & Ross, A. J. Amberground pholadid bivalve borings and inclusions in Burmese amber: implications for proximity of resin-producing forests to brackish waters, and the age of the amber. *T. Roy. Soc. Edin-Earth.* **107**, 239–247 (2018).
42. Feng, Y.-J. *et al.* Phylogenomics reveals rapid, simultaneous diversification of three major clades of Gondwanan frogs at the Cretaceous–Paleogene boundary. *P. Natl. Acad. Sci. USA* 114, E5864–5870; 10.1073/pnas.1704632114 (2017).
43. Maglia, A. M. & Púgener, L. A. Skeletal development and adult osteology of *Bombina orientalis* (Anura: Bombinatoridae). *Herpetologica* **54**, 344–363 (1998).
44. Haas, A. Larval and metamorphic skeletal development in the fast developing frog *Pyxicephalus adspersus* (Anura, Ranidae). *Zoomorphology* **119**, 23–35 (1999).
45. Duellman, W. E. & Trueb, L. *Biology of Amphibians*. (John Hopkins University Press, 1994.).
46. Dong, L-P., Roček, Z., Wang, Y. & Jones, M. E. H. Anurans from the Lower Cretaceous Jehol Group of Western Liaoning. *PLoS One* **8**, e69723; 10.1371/ journal.pone.0069723 (2013).
47. Báez, A. M., Moura, G. J. B. & Gómez, R. O. Anurans from the Lower Cretaceous Crato Formation of north-eastern Brazil: implications for the early divergence of neobatrachians. *Cretaceous Res*. **30**, 829–846 (2009).
48. Báez, A. M. Anurans from the Early Cretaceous Lagerstatte of Las Hoyas, Spain: new evidence on the Mesozoic diversification of crown-group Anura. *Cretaceous Res*. **41**, 90–106 (2013).
49. Fregenal-Martinez, M. & Meléndez, N. Environmental reconstruction: a historical review in *Las Hoyas: A Cretaceous Wetland* (eds Poyato-Ariza, F. J. & Buscalioni, A. D.) 14–28 (Verlag Dr. Friedrich Pfeil, 2016).
50. Wang, B. *et al*. Brood care in a 100-million-year-old scale insect. *eLife* 4, e05447; 10.7554/eLife.05447 (2015).
51. Chen, R. C. *et al*. PITRE: software for phase-sensitive X-ray image processing and tomography reconstruction. *J. Synchrotron Radiat*. **19**, 836–845 (2012).

Acknowledgements

We thank Christopher M. Schalk (Sam Houston State University, TX, USA) and Hao Ran (Key Laboratory of Ecology of Rare and Endangered Species and Environmental Protection, Ministry of Education, Guilin, China) for discussion, Shenna Wang (Dexu Institute of Palaeontology,

China) for providing the specimens for study. This research was funded by the National Natural Science Foundation of China (No. 41790455, 41772008), the National Geographic Society, USA (No. EC0768-15), the Fundamental Research Funds for the Central Universities (No. 2652017215), the State Key Laboratory of Palaeobiology and Stratigraphy (Nanjing Institute of Geology and Palaeontology, Chinese Academy of Sciences) (No. 173127), and the Natural Sciences and Engineering Research Council of Canada (2015-00681).

Author Contributions

L.X. and S.E. designed the project. L.X. and H.C. acquired the specimen, supervised, and conducted the initial analytical work. D.W. performed the earlier analyses. G.L. and M.B. scanned and interpreted the data. L.X., D.W., R.M., and S.E. wrote the manuscript. L.X., D.W., and S.E. contributed equally to the completion of the manuscript, analyses, and images.

The authors declare no competing interests.

Tables

Table 1 Measurements (in mm) of egg masses from mid-Cretaceous Burmese amber

Table 2 Measurements (in mm) of eggs from mid-Cretaceous Burmese amber

Table 3 The measurements of intact eggs from mid-Cretaceous Burmese amber (mm).

Figure legends

Figure 1 Egg masses in amber from Myanmar. A, Morphotype 1 DIP-V-16122; B, Morphotype 2 DIP-V-17227.

Figure 2 Egg masses rendered in 3D from CT scans. A, Morphotype 1 DIP-V-16122, six views; B, Morphotype 2 DIP-V-17227, six views.

Figure 3 DIP-V-16122, Morphotype 1 egg mass, a series of slices through the egg mass to show: A, the external surface; B-D, the distortion in shape of the eggs within the mass; and B-E, the husk-like eggs in the lower part of the mass. Small black arrows in B and C indicate small cavities within individual eggs; white arrows in C and D indicate the husk-like eggs.

Figure 4 DIP-V-16122. A, Enlargement of Morphotype 1 egg mass showing possible areas of fungal growth, further enlarged in B and C.

Figure 5 DIP-V-17227. Morphotype 2 egg mass, a series of slices through the egg mass to show A, external surface with small protrusions arrowed in black and highly wrinkled surfaces asterisked (*), B-D showing the more solid and less distorted shapes of the eggs within the mass and the laminated appearance in some specimens. White arrows in C and D indicate insect frass.
Figure 6 Egg morphotype 3, interpreted as insect eggs. A-C, DIP-V-17160, in A, within the amber, B, rendered CT image, and C, enlargement of one egg with embryo; D, amber specimen DIP-V-17234; E, amber specimen DIP-V-18106.

Figure 6 Morphotype 3 egg masses, interpreted as insect eggs. A-C, DIP-V-17160, in A, within the amber, B, rendered CT image, and C, enlargement of one egg with embryo; D, amber specimen DIP-V-17234; E, amber specimen DIP-V-18106.

Figure 7 Taphonomic observations with UV light. A,B, DIP-V-16122 eggs and plant fragments intruding on a preexisting resin flow (toward top of image), specimen in same view as Fig. 1A, and reverse, respectively; C, DIP-V-17160 multilayered flow; D,E, DIP-V-17227 stalactite-like flows with eggs at their center, under transmitted light and UV light, respectively; F, DIP-V-17234, multiple laminar flows with extensive oxidation between layers. White asterisks mark position of egg masses, black arrows mark organics (plant fragments and insect frass), white arrows mark oxidized drying lines, and banding within the amber outlines individual flows.

Table 1 Measurements (in mm) of egg masses from mid-Cretaceous Burmese amber

	Size of amber (mm)	Size of egg mass (mm)	Weight (g)
DIP-V-16122	13.0 × 9.0 × 5.0	5.7 × 5.0 × 2.4	0.45
DIP-CH-17227	28.5 × 24.5 × 7.5	4.8 × 3.6 × 2.3	3.08
DIP-V-17160	24.8 × 15.6 × 7.2	9.9 × 4.3 × 0.5	1.64
DIP-V-17234	33.2 × 22.1 ×6.4	9.2 × 3.9 × 0.4	2.51
DIP-V-18106	11.5× 10.6 ×3.72	9.2 × 4.1 × 0.4	0.30

Table 2 Measurements (in mm) of eggs from mid-Cretaceous Burmese amber

Eggs	Quantity	Minimum	Maximum	Average	Median
DIP-V-16122	55	0.84	1.50	1.14	1.11
DIP-CH-17227	35	0.66	0.99	0.83	0.82
DIP-V-17160*	28	1.00| 0.42	1.54| 0.75	1.29| 0.59	1.34| 0.59
DIP-V-17234*	18	0.95| 0.45	1.71| 0.84	1.42| 0.63	1.46| 0.63
DIP-V-18106*	22	0.89| 0.47	1.43| 0.69	1.17| 0.61	1.20| 0.63

* Dual entries refer to the long axis | short axis of the eggs.

Table 3 The measurements of intact eggs from mid-Cretaceous Burmese amber (mm).

Eggs			Yolk		Percentage
Long axis	Short axis	L/S	Long axis	Short axis	
DIP-V-16122					
1.392	1.049	1.326	0.348	0.317	7.6%

1.264	0.920	1.373	0.378	0.350	11.4%
1.258	1.058	1.189	0.279	0.272	5.7%
1.228	1.073	1.144	0.270	0.267	5.5%
1.375	1.047	1.313	0.242	0.215	3.6%
1.496	1.140	1.313	0.321	0.304	5.7%
1.029	1.001	1.028	0.213	0.202	4.2%
1.474	1.407	1.047	0.327	0.287	4.5%
1.470	1.350	1.089	0.287	0.272	3.9%
1.460	1.203	1.214	0.256	0.237	3.5%
1.310	1.281	1.023	0.272	0.257	4.2%
0.925	0.824	1.122	0.175	0.166	3.8%
0.985	0.884	1.115	0.188	0.169	3.6%
1.076	1.049	1.026	0.223	0.184	3.6%
1.260	1.131	1.114	0.241	0.238	4.0%
0.859	0.802	1.071	0.171	0.159	3.9%
0.865	0.778	1.111	0.165	0.155	3.8%
DIP-CH-17227					
0.869	0.830	1.04	0.378	0.375	20.5%
0.693	0.537	1.29	0.232	0.214	13.3%
0.898	0.860	1.04	0.427	0.356	19.7%
DIP-V-17160					
1.361	0.508	2.680	0.654	0.344	32.5%
1.335	0.751	1.777	0.715	0.314	22.4%
1.184	0.526	2.252	0.844	0.376	51.1%
1.002	0.420	2.387	0.658	0.267	41.8%
1.399	0.654	2.139	0.712	0.312	24.3%
1.241	0.712	1.744	0.564	0.269	17.2%
1.536	0.593	2.589	0.882	0.393	38.0%
1.151	0.516	2.231	0.897	0.447	67.5%
1.429	0.593	2.411	1.101	0.365	47.5%
DIP-V-17234					
1.503	0.629	2.390	1.412	0.527	78.8%
1.407	0.549	2.562	1.395	0.520	94.0%
1.324	0.657	2.016	1.334	0.470	72.1%
0.948	0.446	2.127	0.845	0.376	75.2%
1.714	0.841	2.037	1.599	0.757	83.9%
1.626	0.615	2.643	1.484	0.529	78.5%
1.380	0.677	2.037	1.359	0.643	93.5%
1.455	0.663	2.195	1.337	0.598	82.9%
1.463	0.604	2.422	1.416	0.590	94.5%
DIP-V-18106					
1.200	0.666	1.802	1.056	0.607	80.2%
1.181	0.627	1.883	1.114	0.552	83.1%
1.110	0.603	1.841	0.945	0.466	65.8%
0.978	0.472	2.072	0.775	0.424	71.2%
1.433	0.686	2.089	1.308	0.616	82.0%

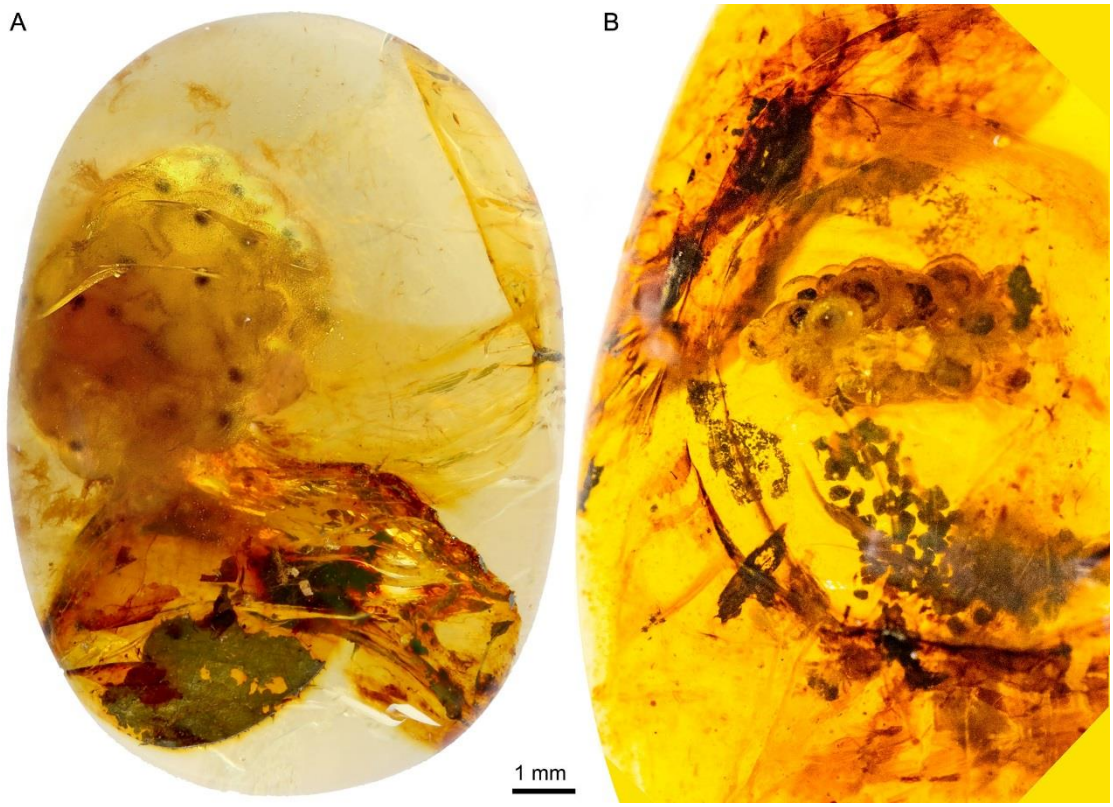

Figure 1 Egg masses in amber from Myanmar. A, Morphotype 1 DIP-V-16122; B, Morphotype 2 DIP-V-17227.

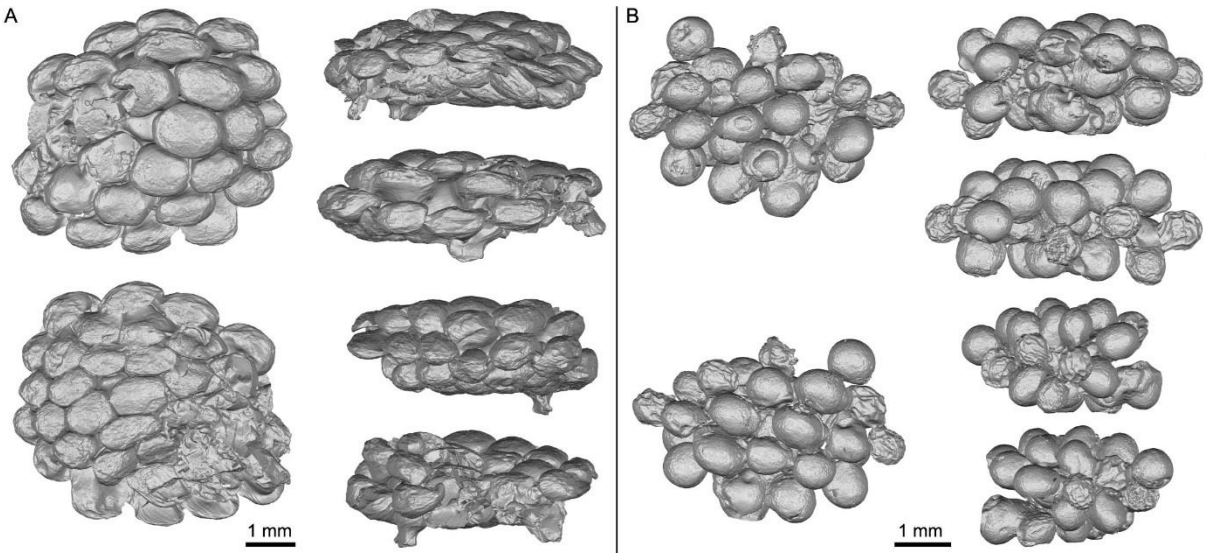

Figure 2 Egg masses rendered in 3D from CT scans. A, Morphotype 1 DIP-V-16122, six views; B, Morphotype 2 DIP-V-17227, six views.

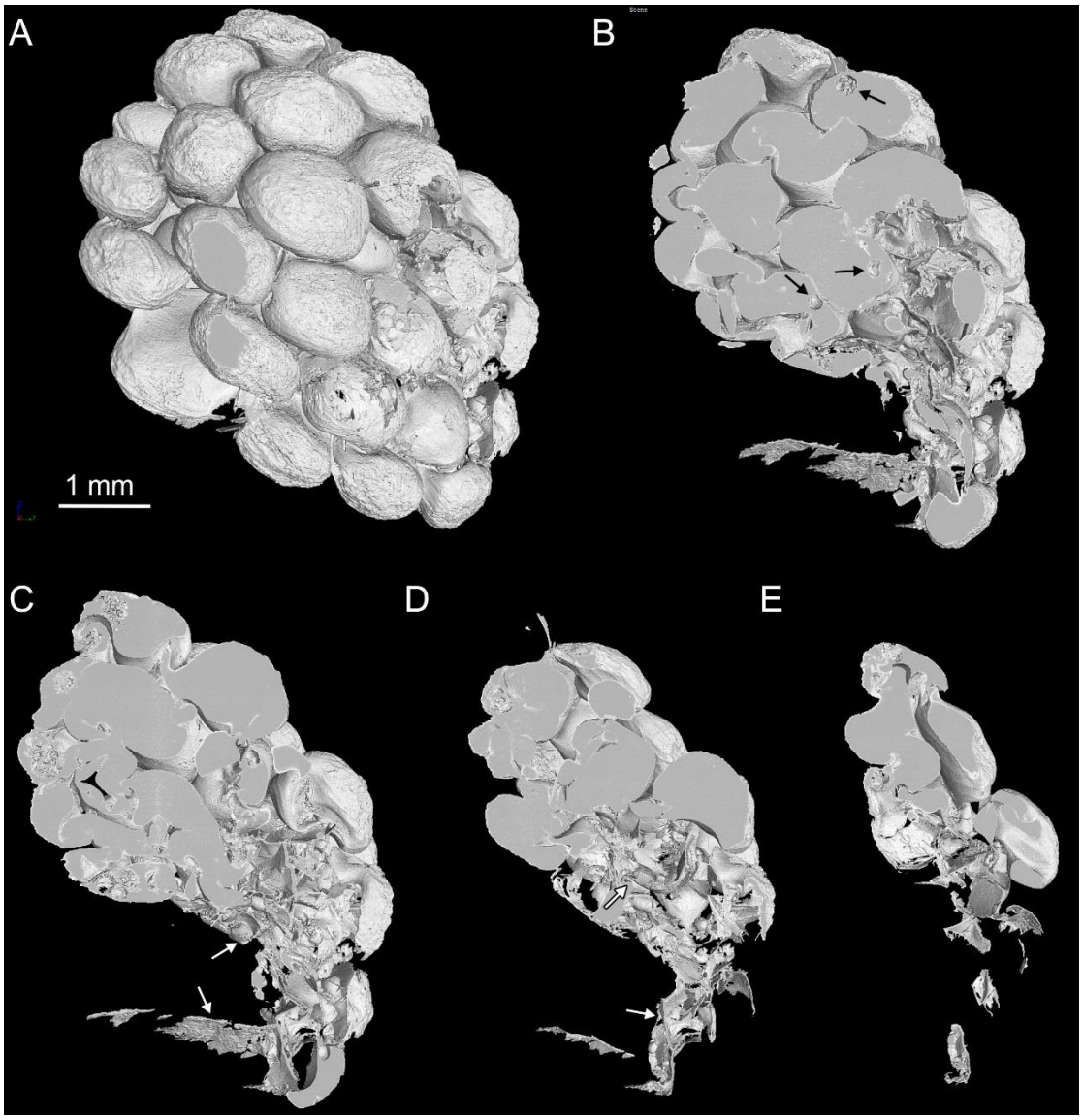

Figure 3 DIP-V-16122, Morphotype 1 egg mass, a series of slices through the egg mass to show: A, the external surface; B-D, the distortion in shape of the eggs within the mass; and B-E, the husk-like eggs in the lower part of the mass. Small black arrows in B and C indicate small cavities within individual eggs; white arrows in C and D indicate the husk-like eggs.

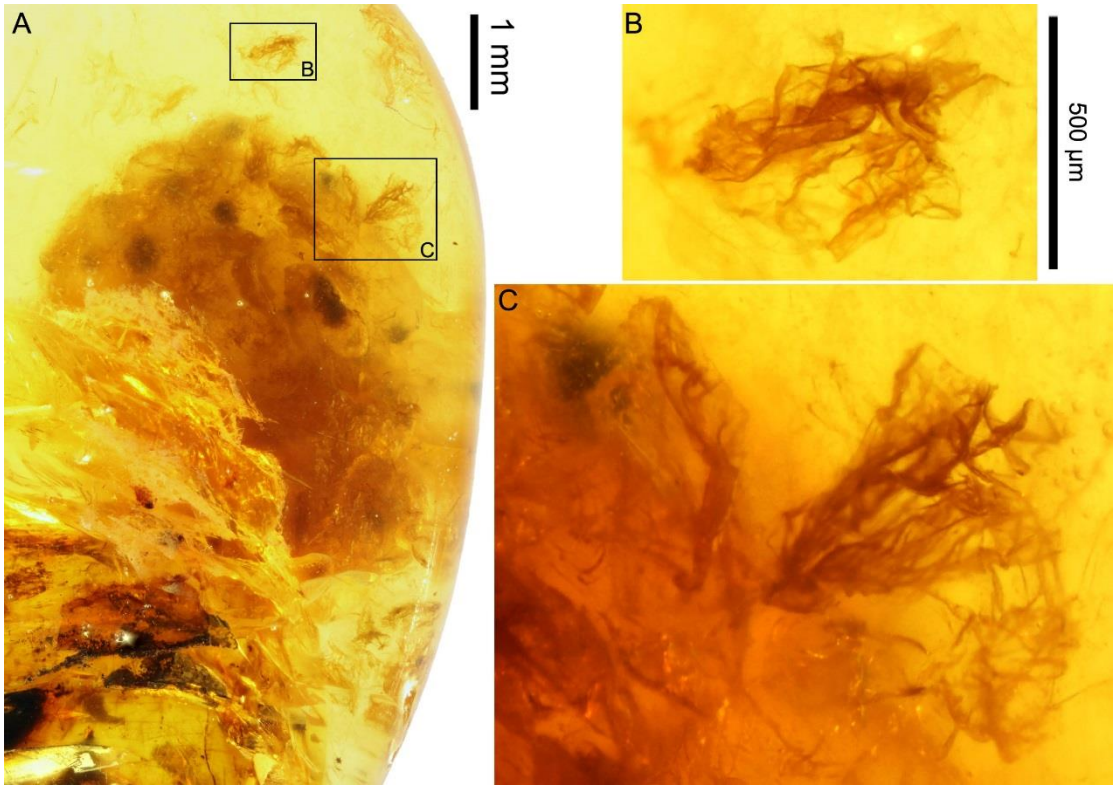

Figure 4 DIP-V-16122. A, Enlargement of Morphotype 1 egg mass showing possible areas of fungal growth, further enlarged in B and C.

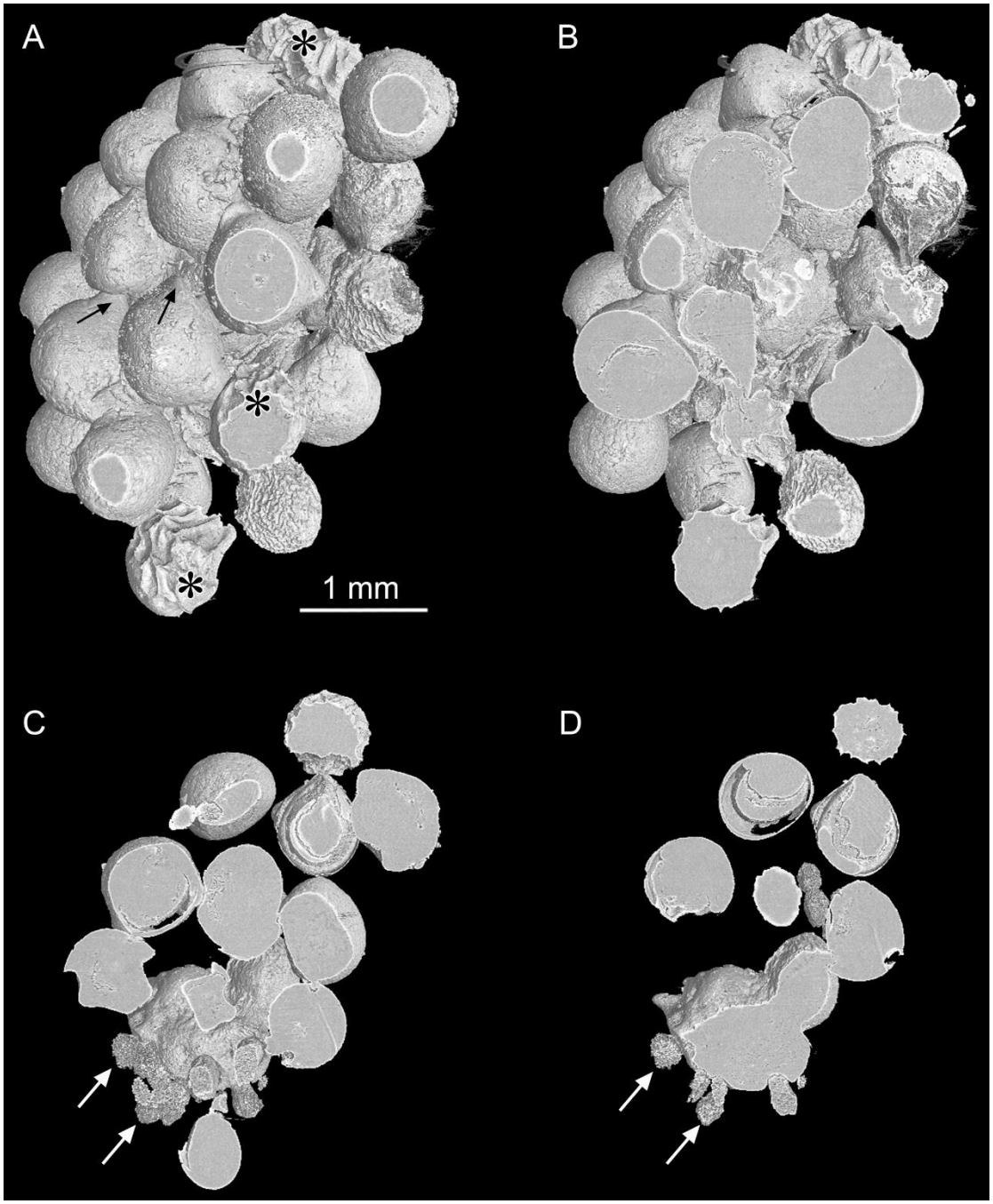

Figure 5 DIP-V-17227. Morphotype 2 egg mass, a series of slices through the egg mass to show A, external surface with small protrusions arrowed in black and highly wrinkled surfaces asterisked (*), B-D showing the more solid and less distorted shapes of the eggs within the mass and the laminated appearance in some specimens. White arrows in C and D indicate insect frass.

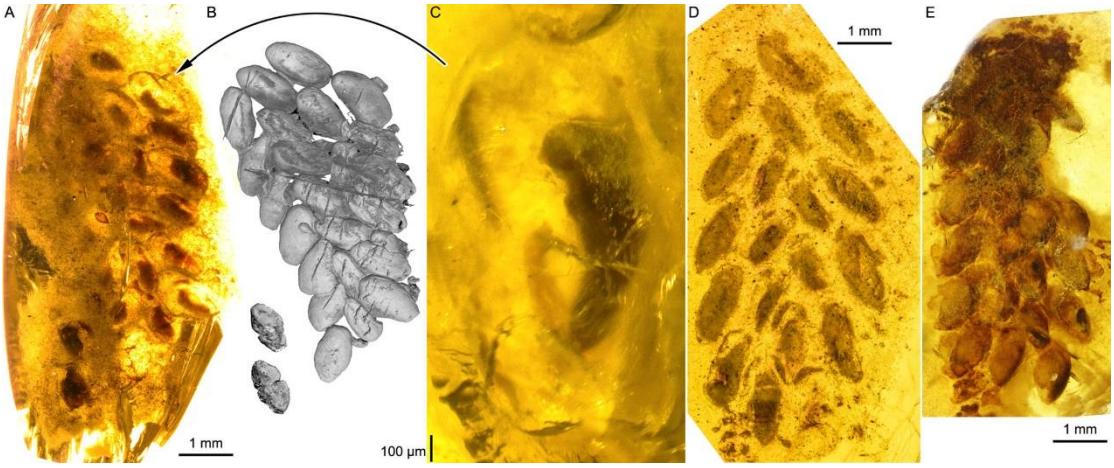

Figure 6 Morphotype 3 egg masses, interpreted as insect eggs. A-C, DIP-V-17160, in A, within the amber, B, rendered CT image, and C, enlargement of one egg with embryo; D, amber specimen DIP-V-17234; E, amber specimen DIP-V-18106.

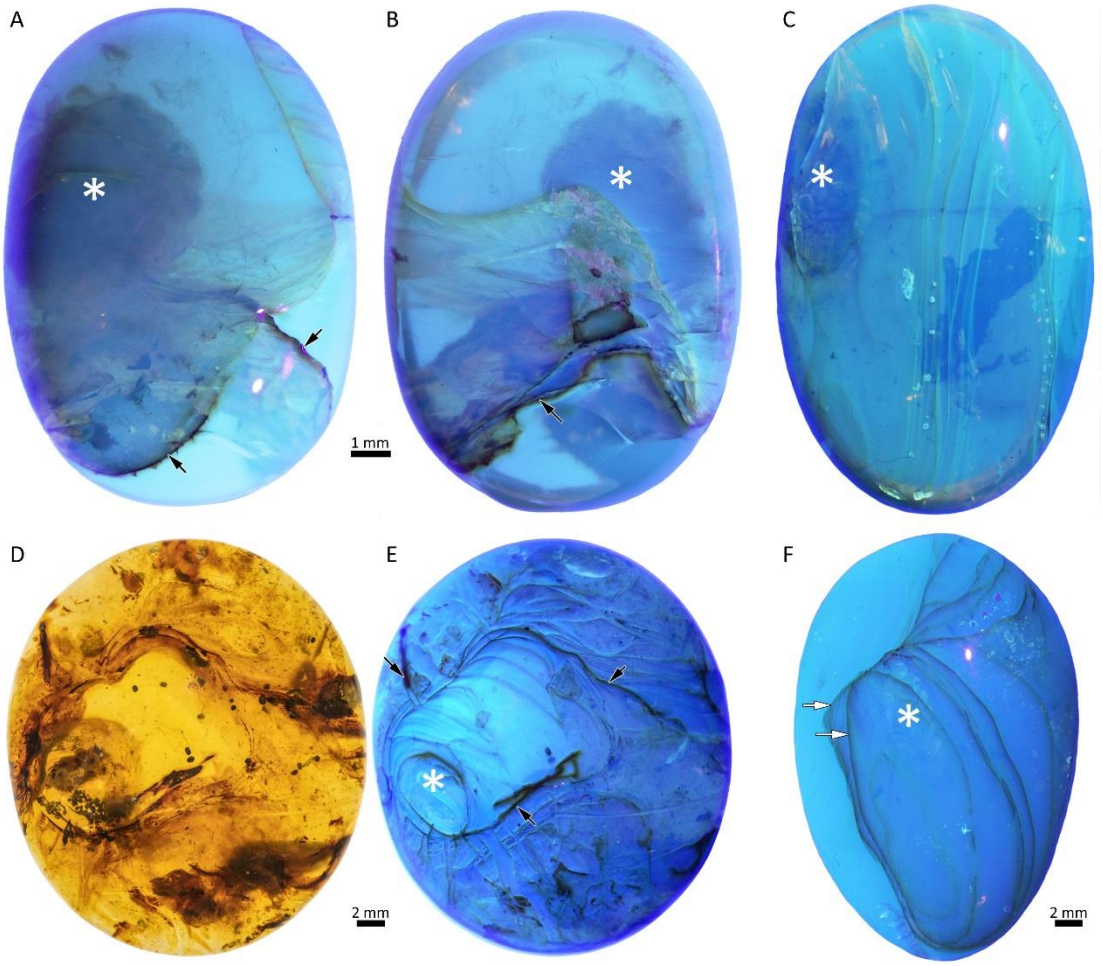

Figure 7 Taphonomic observations with UV light. A,B, DIP-V-16122 eggs and plant fragments intruding on a preexisting resin flow (toward top of image), specimen in same view as Fig. 1A, and reverse, respectively; C, DIP-V-17160 multilayered flow; D,E, DIP-V-17227 stalactite-like flows with eggs at their center, under transmitted light and UV light, respectively; F, DIP-V-17234, multiple laminar flows with extensive oxidation between layers. White asterisks mark

position of egg masses, black arrows mark organics (plant fragments and insect frass), white arrows mark oxidized drying lines, and banding within the amber outlines individual flows.